Diamond & Related Materials 108 (2020) 107923

Contents lists available at ScienceDirect

Diamond & Related Materials

journal homepage: www.elsevier.com/locate/diamond

Structural and mechanism study on enhanced thermal stability of hydrogenated diamond-like carbon films doped with Si/O

Dong Zhang[a,b,1], Shuyu Li[a,b,1], Xiao Zuo[a], Peng Guo[a], Peiling Ke[a,b,*], Aiying Wang[a,b,*]

[a] Key Laboratory of Marine Materials and Related Technologies, Zhejiang Key Laboratory of Marine Materials and Protective Technologies, Ningbo Institute of Materials Technology and Engineering, Chinese Academy of Sciences, Ningbo 315201, China

[b] Center of Materials Science and Optoelectronics Engineering, University of Chinese Academy of Sciences, Beijing 100049, China

ARTICLE INFO

Keywords:
a-C:H
a-C:H:Si:O
Thermal stability
Structure evolution
Residual stress

ABSTRACT

a-C:H and a-C:H:Si:O films with two different Si/O co-doping contents had been deposited using a PECVD system by the mixture of C_2H_2 and HMDSO gas. The structure evolution of as-deposited and annealed films had been characterized by the Raman spectroscopy, XPS and FTIR. A progressive increase of sp^2 carbon sites and a reduction of sp^3 with the increase of the annealing temperature were expected. However, the Si/O co-doping was found to be able to reduce the graphitization degree of the annealed films. After annealing at 400 °C, the decrease rate of sp^3 fraction of a-C:H film was 14.2%, while the a-C:H:Si:O (0.93 at.% Si) film was 8.16% and the a-C:H:Si:O (3.62 at.% Si) film was 6.8%. To understand the mechanism on the improved thermal stability by Si/O co-doping, the structure and residual stress of the a-C:H and a-C:H:Si:O films were analyzed. The results revealed that silicon atoms were incorporated into the carbon network by substituting carbon atoms of the films, which had also been characterized contributed to produce the C—Si sp^3 bonds stabilized by the oxygen. Residual stress characterization also demonstrated that, the residual stress of the a-C:H:Si:O films was greatly reduced compared with that of the a-C:H films. Therefore, the fraction of the highly strained C—C sp^3 bonds, which were more likely to break at elevated temperature, was reduced in the a-C:H:Si:O films. This kind of structure evolution endowed the a-C:H:Si:O films higher hardness and adhesion at high temperature.

1. Introduction

Over the last few decades, diamond-like carbon (DLC) films have been successfully used in a wide range of technological applications, including as protective coatings for machining tools, moulds and moving components [1–3]. In spite of DLC films owning a series of excellent properties such as high hardness, wear resistance and self-lubrication, the limited thermal stability is still a barrier for the wider use of DLC films [4–6]. Different with hydrogen free amorphous carbon films, hydrogenated DLC (a-C:H) presents a poor thermal stability which is less than 300 °C [7,8]. In general, a-C:H is composed of an amorphous matrix of C—C bonding hybridized in the sp^2 and sp^3 configuration, together with a fraction of C—H sp^3 bonding. Hydrogen provides a means to terminate dangling carbon bonds and stabilize sp^3 bonding [9]. However, at elevated temperatures, degradation occurs more likely through the scission of C—H sp^3 bonds resulting in a progressive increase in the fraction of sp^2-bonded carbon in the films. For example, in the case of temperatures relevant technology like hot working die, high-speed cutting toll and protective coatings on components in car engines, a-C:H rapidly degrades [10,11].

Introducing various metal or nonmetal elements has been considered as promising strategy to modify the compressive stress and tribological characteristics of a-C:H [12–17]. Especially, two or more elements co-doping has been taken into account to reduce the residual compressive stress while not significantly affecting the mechanical properties and provide the desirable tribological properties [18,19]. Our previous research showed that the Ti/Al or Cu/Cr co-doped a-C:H films exhibited low residual stress, high hardness, good toughness, as well as low coefficient of friction and wear rate, which was attributed to the combination of weak bonding and antibonding interactions [20–22]. It has been demonstrated that the co-doping with silicon and oxygen elements into a-C:H presents other interesting properties, such as enhanced thermal stability, improved optical characteristics and good tribological behavior (i.e., low friction and wear) across a broader

* Corresponding authors at: Key Laboratory of Marine Materials and Related Technologies, Zhejiang Key Laboratory of Marine Materials and Protective Technologies, Ningbo Institute of Materials Technology and Engineering, Chinese Academy of Sciences, Ningbo 315201, China.

E-mail addresses: kepl@nimte.ac.cn (P. Ke), aywang@nimte.ac.cn (A. Wang).

[1] These authors contributed equally to this work and should be considered as co-first authors.

https://doi.org/10.1016/j.diamond.2020.107923
Received 24 March 2020; Received in revised form 8 May 2020; Accepted 9 May 2020
Available online 13 May 2020

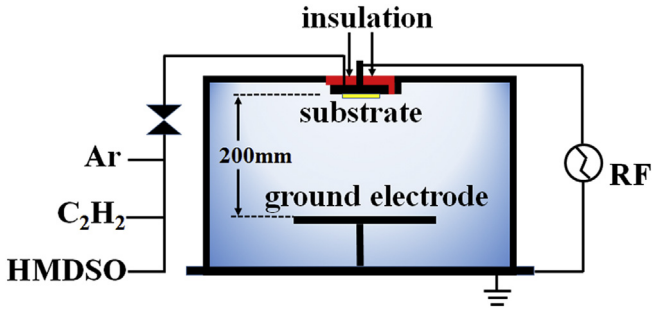

Fig. 1. Schematic diagram of PECVD system.

range of conditions and environments [23–25]. S.M. Baek [26] showed SiOx-DLC films favorable feature of high deposition rate and large optical band gap although higher O/C ratio brought about poor adhesion strength of the films. S. Bhowmick and A.T. Alpas [27] examined the a-C:H/a-Si:O films maintained the low room temperature(25 °C) steady state COF (μ_s of 0.17) up to 400 °C while a-C:H films typically showed high COF. F. Mangolini [28] demonstrated that the a-C:H:Si:O films grown by plasma-enhanced chemical vapor deposition (PECVD) with silicon and oxygen levels of, respectively, 6 ± 1 at.% and 3 ± 1 at.% exhibited a slightly-enhanced thermal stability under high vacuum conditions compared to a-C:H. In the literature it is proposed that a-C:H:Si:O consists of two amorphous interpenetrating networks, a diamond-like network of amorphous carbon and hydrogen (a-C:H) and a second amorphous silica network (a-Si:O) [29,30]. Yet the influence of silicon and oxygen on the thermally induced structural evolution of a-C:H:Si:O films in atmosphere still needs further systematic study. Previous studies have shown that Si/O co-doping hydrogenated DLC (a-C:H:Si:O) has significantly higher thermal stability than a-C:H, however, why the inclusion of silicon and oxygen results in such increases in thermal stability has not yet been explored.

In this paper, a-C:H film and a-C:H:Si:O films with different Si/O co-doping contents were synthesized by PECVD. The structure evolution of these films annealing in various temperatures was evaluated. Effect of Si/O co-doping on the structure and residual stress of different films were investigated, in order to understand the mechanisms by which inclusion of silicon and oxygen achieved higher thermal stability.

2. The Experimental details

2.1. The coating deposition processes

The films were deposited by PECVD system. It consisted of a cylindrical chamber of 350 mm in diameter and 300 mm in length. There were a RF power electrode on top used as substrate holder and a ground electrode underneath of 50 mm and 170 mm in diameter respectively, the distance between them was 200 mm (Fig. 1). RF power was coupled to the electrode by a 13.56 MHz RF generator through an impedance matching unit. Acetylene (C_2H_2) and hexamethyl disiloxane (HMDSO) were used as the precursor gas. A steel container containing liquid HMDSO was heated to 50–70 °C in a water bath and a constant vapor supply of HMDSO was delivered during deposition. The stainless steel tubing connecting the vessel containing the liquid precursor to the chamber was heated to 70–90 °C to prevent condensation. The gas flow rates were controlled by respective mass flow controllers and mixed before they entered the deposition chamber with different mixture ratio. Mirror polished Si (100) and cemented carbide substrates were used for deposition. They were ultrasound cleaned with alcohol and dried with nitrogen. Cleaned substrates were fixed on the substrate holder. Deposition system were evacuated to a base pressure of 2.0×10^{-3} Pa. Initially, the substrates were cleaned in Ar plasma for 30 min. Then the a-C:H and a-C:H:Si:O films were deposited with different gas mixture ratio as shown in Table 1. During the deposition of the three films, the RF power was set at 100 W, pressure was 2 Pa, and deposition time was for 30 min. After deposition, the deposited films were heated in air condition to the annealing temperature at 100, 200, 300, 400 and 500 °C respectively, with a heating rate of 10 °C/min. The samples were kept at the certain temperature for 2 h and then cooled inside the furnace to room temperature.

2.2. Characterization details

A surface profilometer (Alpha-step IQ, USA) was used to measure the thickness of the deposited films with employing a step formed by a shadow mask. Raman spectroscopy (inVia-reflex, Renishaw) with 532 nm excitation was employed to evaluate the carbon atomic bonds of the films. The chemical composition and bonds of the films were characterized by X-ray photoelectron spectroscopy (XPS, Axis UltraDLD, Japan) with Al (mono) Kα radiation. The chemical structure of the films was characterized with FTIR spectroscopy (Thermo, Nicolet 6700). To exclude IR absorption from substrates, a piece of Si (100) wafer was used as the substrate for investigating FTIR spectroscopy. The residual stress was calculated according to the Stoney equation and the film/substrate curvature determined by a laser tester (JLCST022, J& L Tech). The hardness (H) was evaluated using a load-controlled (MTS NANO G200) nanoindentation equipped with a Berkovich diamond indenter with a tip radius of approximately 150 nm. The characteristic H was chosen in a depth of around 1/10 of the film thickness, where the measured value was not affected greatly by the substrate. Five indents were made on each film samples to evaluate the average H from load–displacement curves using the Oliver-Pharr method. The adhesion of the films on cemented carbide substrates was evaluated with scratch tester (CSM, Revetes) with diamond tip (radius 10 μm). The sliding load increased from 1 N to 100 N, and the sliding speed was fixed at 0.1 mm/s. The critical load (Lc_1) was defined as the lowest load at which the films started to delaminate from substrates.

3. Results and discussion

3.1. Thermally induced structural evolution

The thickness and deposition rate of the a-C:H and a-C:H:Si:O films are shown in Fig. 2. When only pure C_2H_2 is used as the precursor gas, the thickness of the film is about 725 nm, and the deposition rate is 24.2 nm·min^{-1}. The ratio of C_2H_2 to HMDSO is 3:1 at the case of mixture, meanwhile the film thickness increases to about 1072 nm, and the deposition rate increases to 35.7 nm·min^{-1}. When the ratio of C_2H_2 to HMDSO is 2:1, the thickness of the film increases to about 1153 nm, and the deposition rate increases to 38.4 nm·min^{-1}. It is obvious that

Table 1
Deposition parameters and composition of the films.

Film number	Gas flow rate/sccm		C concentration (at.%)		Si concentration (at.%)		O concentration (at.%)	
	C_2H_2	HMDSO	As-deposited	Annealed (400 °C)	As-deposited	Annealed (400 °C)	As-deposited	Annealed (400 °C)
DLC	30	0	97.69	97.45	0	0	2.31	2.55
SiOx-DLC-1	30	10	96.69	96.32	0.93	0.94	2.38	2.74
SiOx-DLC-2	30	15	92.63	92.09	3.62	3.57	3.75	4.34

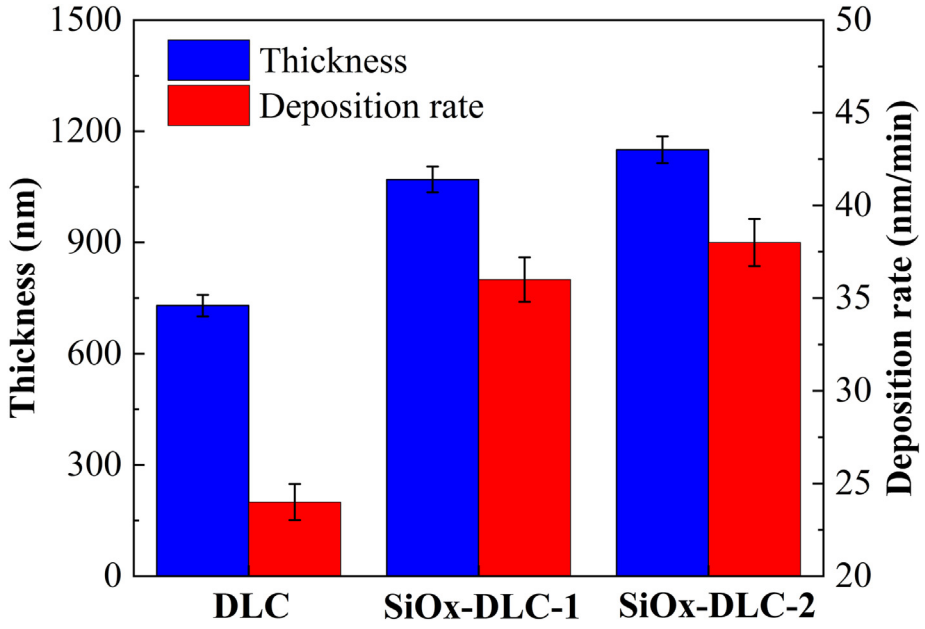

Fig. 2. Thickness and deposition rate of different films.

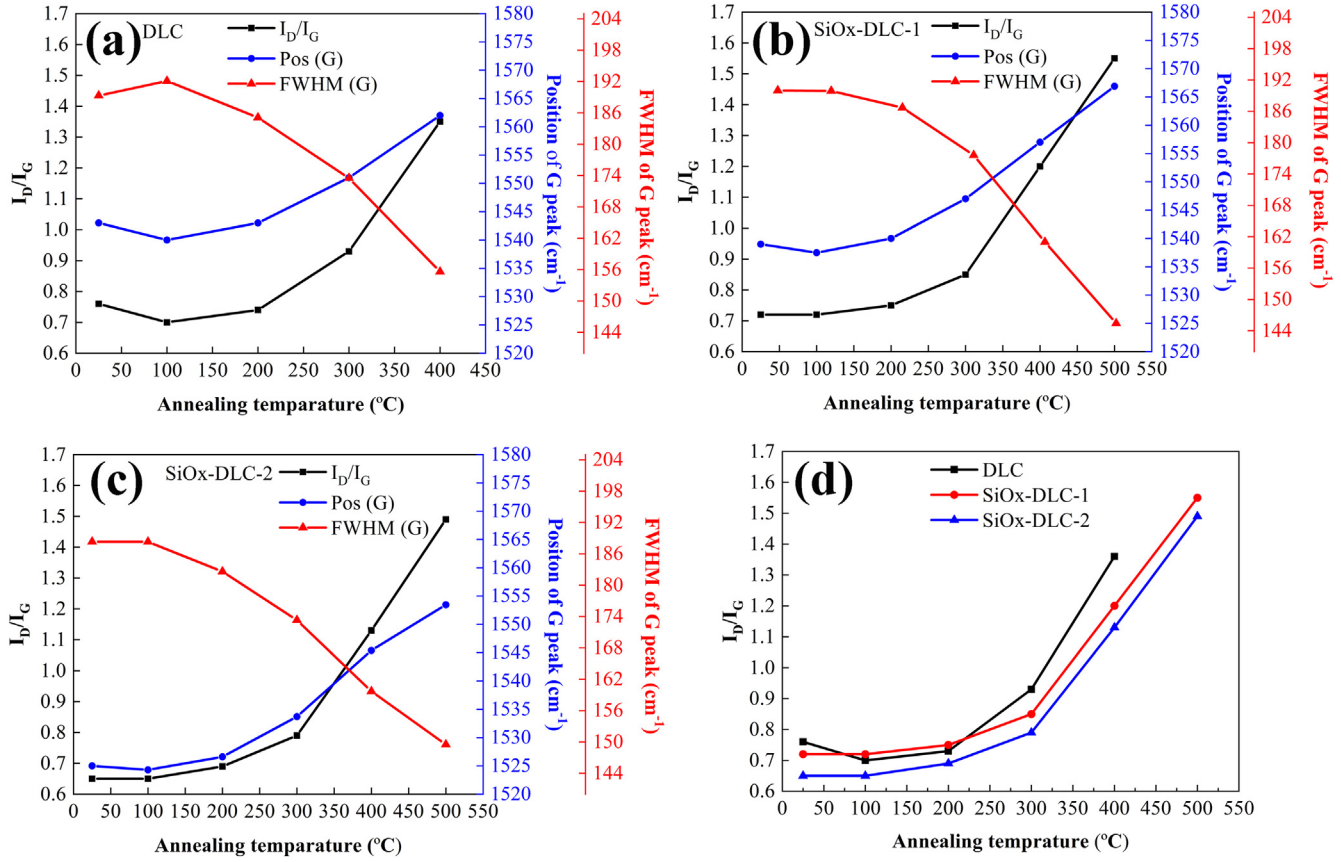

Fig. 3. Raman spectra fitting analysis of different films annealed at various temperatures (a) DLC (b) SiOx-DLC-1 (c) SiOx-DLC-2 (d) comprehensive analysis.

the introduction of HMDSO can improve the deposition rate of the films. Due to the ionization energy of HMDSO is lower than C_2H_2, the increase of dissociation rate of reaction gas with more HMDSO is expected. With the increase of HMDSO content in the reaction gas, the self-bias voltage of the substrate decreases from about 750 V to 680 V under the same RF power supply of 100 W, indicating the increase of ion current for film-forming, consequently the increase of deposition rate is produced.

The chemical composition of the as-deposited and annealed films at 400 °C is measured by XPS and given in Table 1. The DLC film is mainly composed of carbon and contains a small amount of oxygen of about 2.31 at.%. The oxygen in the film either comes from the film oxidation due to air exposure after deposition, or is incorporated during the film growth owing to water and gas released from the reactor walls. In the

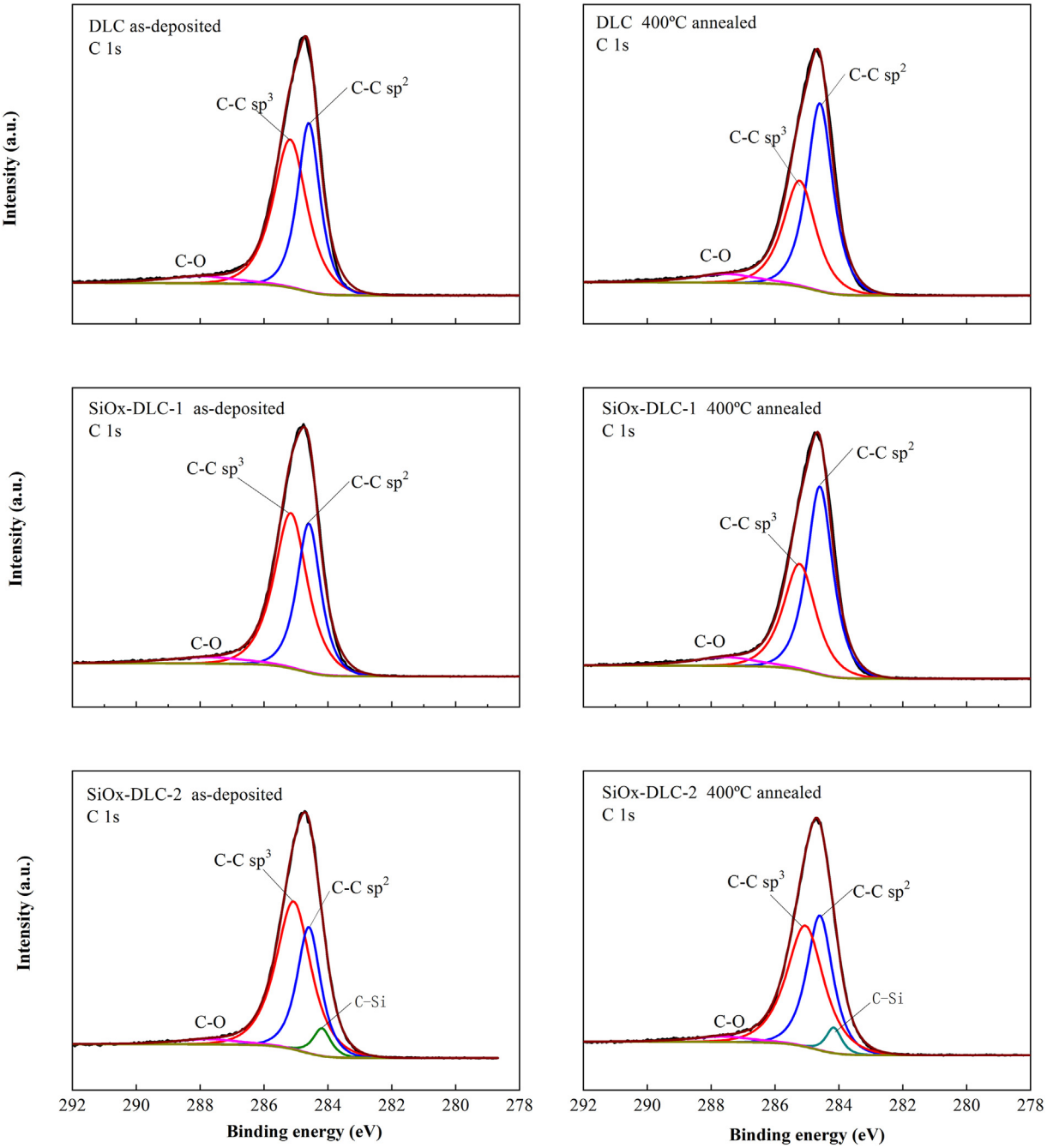

Fig. 4. XPS spectra for C 1s core electrons of different films as-deposited and annealed at 400 °C.

case of SiOx-DLC-1 and SiOx-DLC-2, these two films are mainly composed of carbon element, and a small amount of silicon and oxygen are incorporated in the films. The atomic percentage of silicon and oxygen in the SiOx-DLC-1 film is 0.93% and 2.38% respectively, and increases to 3.62% and 3.75% in the SiOx-DLC-2 film. After annealed at 400 °C, the composition of the carbon and silicon in the three films does not change significantly, except that the composition of the oxygen increases slightly indicating the slight oxidation of the films.

Raman spectra of all samples present a broad asymmetric Raman scattering band in the range of 1000–1700 cm^{-1}, which are essentially as same as the typical carbon bond structure in a-C:H films [9]. The spectra curves of the films are fitted with two Gaussian peaks simulating D (in the vicinity of 1350 ± 30 cm^{-1}) and G (in the vicinity of 1550 ± 30 cm^{-1}) peaks [31–33]. According to the fitted G-peak position, the intensity ratio of D peak to G peak (I_D/I_G) and the full width at half maximum (FWHM) of G-peak, the bonding structure of DLC films such as bond disorder, sp^3/sp^2 ratio, sp^2 site clustering can be derived qualitatively. Fig. 3a–c presents the Raman spectra fitting analysis of the three films annealed at various temperatures. When the temperature is lower than 200 °C, the I_D/I_G, position and FWHM of G peak of the three films have no obvious change, indicating that the structure is relatively stable. When the temperature arising from 200 °C to 500 °C, the I_D/I_G increases, G-peak shifts upwards and the FWHM of G peak decreases upon annealing for all films. The a-C:H film completely peels off from the substrate after 500 °C annealing, due to the hydrogen desorption from the edges of the sp^2 dominated clusters. Generally, the decrease of the sp^3 bonding fraction will cause the G-peak position to shift upwards and the I_D/I_G ratio will increase in hydrogenated DLC films. The decrease of FWHM (G) which describes structural disorder of the films is related to the decrease of sp^3 content.

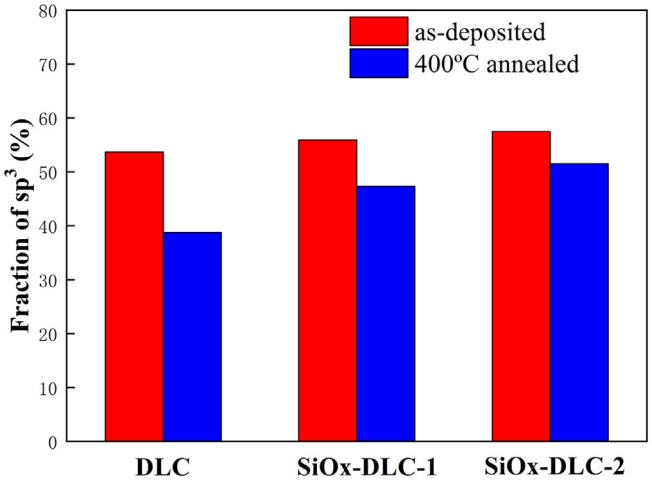

Fig. 5. The fitting results about sp^3 fraction of different films as-deposited and annealed at 400 °C.

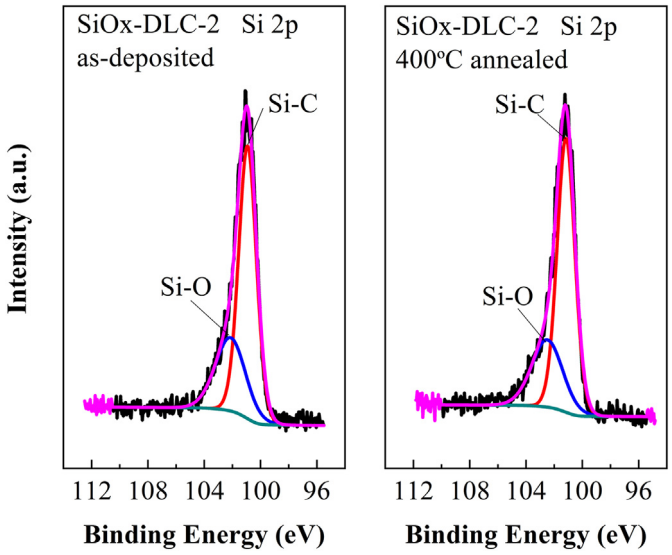

Fig. 6. XPS spectra for Si 2p core electrons of SiOx-DLC-2 film as-deposited and annealed at 400 °C.

Raman analysis curves of the three films implying a progressive clustering and increasing of the sp^2 carbon sites together with a reduction of sp^3 with annealing temperature rising [34]. This indicates that annealing leads to graphitization of the a-C:H and a-C:H:Si:O films. The change of I_D/I_G with the increase of annealing temperature of the three films is plotted in Fig. 3d. It shows that the order of growth rate of I_D/I_G is DLC, SiOx-DLC-1 and SiOx-DLC-2, which indicates that Si/O co-doping is beneficial to reduce graphitization of a-C:H films caused by thermal treatment.

XPS spectra for C 1s core electrons of the three films as-deposited and annealed at 400 °C are illustrated in Fig. 4. In each C 1s spectrum, the peak shape is similar and there is a major peak presented at 284.6 eV, attributing to the amorphous carbon structure. For DLC film, the C 1s spectrum can be divided into three peaks, which correspond to the sp^3-C bond near 285.2 eV, sp^2-C bond near 284.4 eV, C—O bond near 286.5 eV. Due to the low silicon content in SiOx-DLC-1 film, it is difficult to distinguish the C—Si bond, and its peak separation is similar to that of DLC film. SiOx-DLC-2 film has one more dividing peak near 283.4 eV represents the C—Si bond compared with the other two films. The fitting results about sp^3 fraction as shown in Fig. 5 also shows that after annealing at 400 °C, the decrease rate of sp^3 fraction of DLC film is 14.2%, while the SiOx-DLC-1 film is 8.16% and the SiOx-DLC-2 film is 6.8%. This indicates that the increase of Si/O co-doping content is correlated with the increase of thermal stability of the a-C:H:Si:O films. These results are in good agreement with Raman spectroscopy fitting analysis discussed above.

3.2. The mechanism of higher thermal stability of a-C:H:Si:O films

Due to the low silicon content in SiOx-DLC-1 film, it is difficult to distinguish the Si peak in XPS spectra. Fig. 6 shows the XPS spectra for Si 2p core electrons of SiOx-DLC-2 film as-deposited and annealed at 400 °C. The peaks for Si 2p can be resolved into two contributions, one at 101.1 ± 0.1 eV and another at 102.4 ± 0.1 eV. The peak at lower binding energy is consistent with silicon carbide bonds. The one with higher binding energy most likely arises from the presence of silicon bonded to oxygen [35,36]. This shows that silicon in carbon network mainly exists in Si—C structure and forms a small amount of Si—O. No obvious change of peak area ratio of Si—C to Si—O is observed between films as-deposited and annealed at 400 °C. It shows that the structure of Si—C and Si—O bond is stable after annealing.

The FTIR spectrums in the range of 400 to 4000 cm^{-1} of the as-deposited and annealed films are shown in Fig. 7. The absorption peaks centered near 850 cm^{-1} represent Si—C vibrations, the peaks centered between 1080 and 1100 cm^{-1} represent Si—O—Si asymmetric stretching vibrations, and the peaks centered between 2800–3050 cm^{-1} correspond to the stretching mode of C—H bonds [37,38]. From the FTIR spectrums of the three as-deposited films as shown in Fig. 7a, there is only weak C—H peak in DLC film and the peaks corresponding to Si—C, Si—O and C—H are characteristic for SiOx-DLC-1 and SiOx-DLC-2 films. The peaks intensity of SiOx-DLC-2 are stronger than SiOx-DLC-1 due to more silicon and oxygen doping in the film. This indicates that silicon can be incorporated into carbon network substituting carbon atoms and contributing to produce silicon carbide, and the carbon is stabilized by hydrogen while silicon is stabilized by oxygen. Fig. 7b and c show the spectrums of SiOx-DLC-1 and

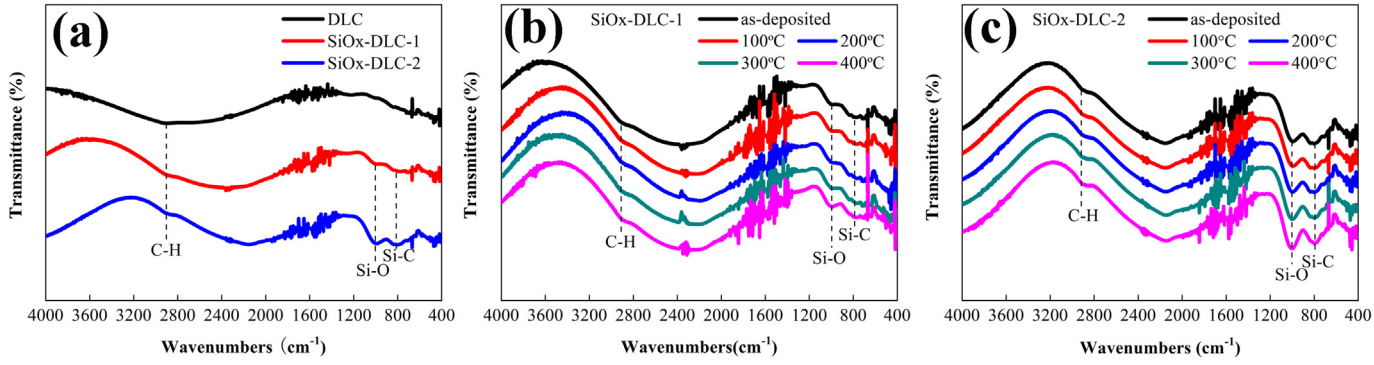

Fig. 7. FTIR spectra of (a) different films as-deposited (b) (c) SiOx-DLC-1 and SiOx-DLC-2 as-deposited and annealed at various temperatures.

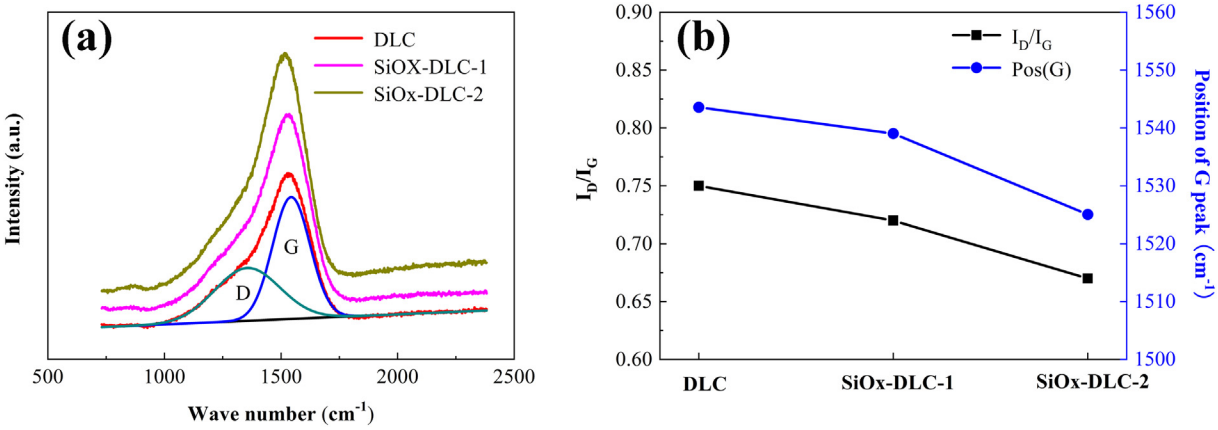

Fig. 8. (a) Raman spectra and (b) fitting analysis of different films as-deposited.

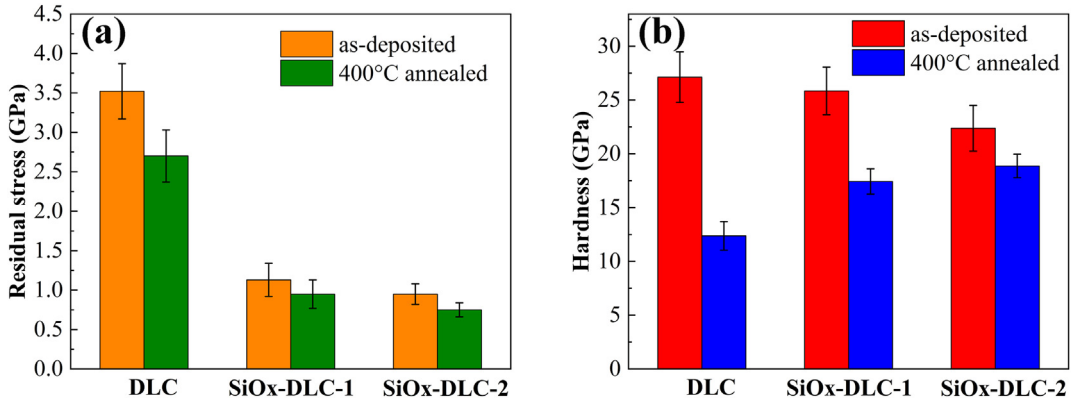

Fig. 9. (a) Residual stress and (b) hardness of different films as-deposited and annealed at 400 °C.

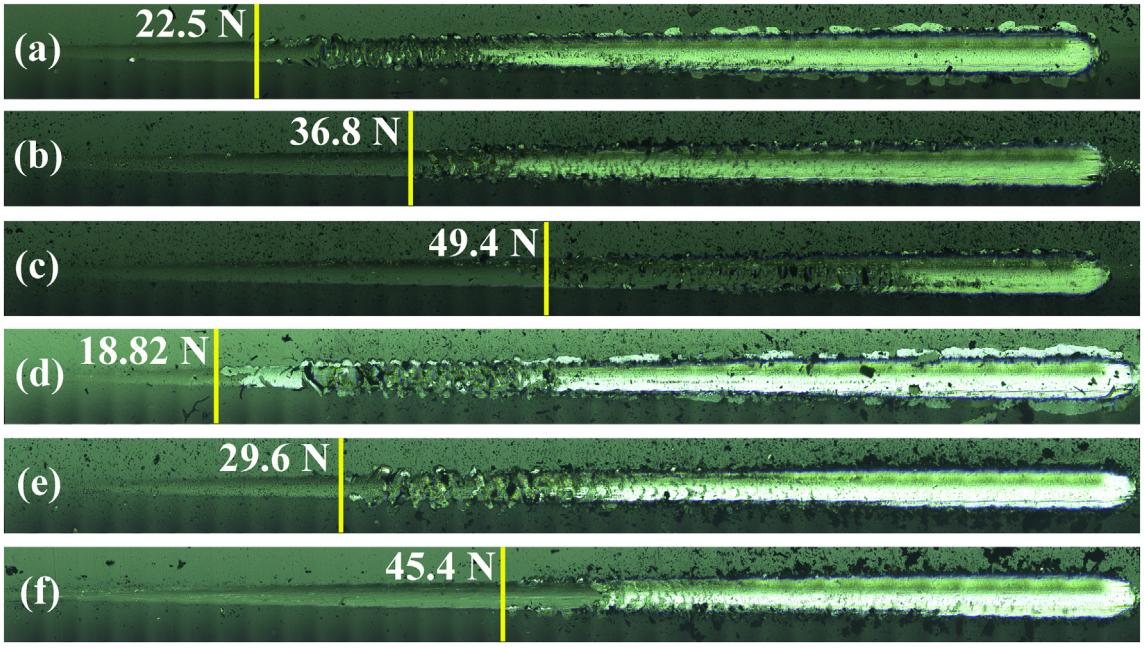

Fig. 10. Scratch morphology on cemented carbide substrates of (a) DLC (b) SiOx-DLC-1 (c) SiOx-DLC-2 films as-deposited and (d) DLC (e) SiOx-DLC-1 (f) SiOx-DLC-2 films annealed at 400 °C.

SiOx-DLC-2 films annealed at different temperature respectively. The intensity of Si—O peaks increases slightly with the increase of annealing temperature, while no significant changes about the Si—C and C—H peaks is observed. This indicates that the structure of silicon carbide in the a-C:H:Si:O films remains stable except that the slight oxidation of silicon after annealing.

Fig. 8a displays the Raman spectra of the as-deposited DLC, SiOx-DLC-1 and SiOx-DLC-2 films. The spectra curves are first treated with a

linear background and then fitted with two Gaussian peaks simulating D (in the vicinity of 1350 ± 30 cm^{-1}) and G (in the vicinity of 1550 ± 30 cm^{-1}) peaks. The G peak is due to the bond stretching of all pairs of sp^2 atoms in both rings and chains. The D peak is due to the breathing modes of sp^2 atoms in rings [31–33]. For the a-C:H films, it is empirically known that the G-peak position will shift upwards and the intensity ratio of the D and G peak (I_D/I_G) will rise as the graphitic fraction in the film increases [39–41]. Fig. 8b shows the variation of I_D/I_G and G peak position of the three films. It should be noted that the I_D/I_G decreases and the G peak shift downwards with the increase of HMDSO in gas mixture. We can conclude that Si/O co-doping reduces the bonding fraction of sp^2 and promotes the formation of sp^3 bonding in the a-C:H:Si:O films. This proves that Si stabilizes the carbon atoms in the sp^3 hybridization state. The superior thermal stability of a-C:H:Si:O compared to a-C:H is suggested to arise from the 4-fold coordination of silicon [42], which stabilizes the carbon atoms in the C—Si sp^3 hybridization state while silicon is stabilized by oxygen (thus inhibiting their conversion into sp^2 -bonded carbon at elevated temperatures).

Fig. 9 shows the residual stress and Hardness of the three films as-deposited and annealed at 400 °C. It can be seen that the residual compressive stress of as-deposited DLC film is as high as 3.52 GPa. With the increase of Si/O co-doping content, the residual stress of SiOx-DLC-1 decreases dramatically to 1.13 GPa, and the residual stress of the SiOx-DLC-2 film decreases to 0.95 GPa. After 400 °C annealing, the stress of all the three films decreases due to the stress release. The hardness of the as-deposited a-C:H film is 27.13 GPa, with the increase of the content of Si/O co-doping, the hardness of the a-C:H:Si:O films decreases due to the decrease of residual stress. After 400 °C annealing, the hardness of the three films all decreases resulting from graphitization at high temperature. Because of the improving thermal stability of the a-C:H film by Si/O co-doping, the hardness of the a-C:H:Si:O films decrease less with the increase of Si/O co-doping contents.

The stress of a-C:H:Si:O films are significantly decreased resulting in the increase of films adhesion on cemented carbide substrates as shown in Fig. 10. For both the as-deposited and 400 °C annealed films, the critical load (Lc_1) of DLC is the lowest, and the films on the scratch edge show brittle flaking due to the large residual stress. The critical load (Lc_1) improves and the brittle edge peeling of the films gradually disappears with the increase of Si/O co-doping content. The critical load (Lc_1) of SiOx-DLC-2 film increases more than twice as much as that of DLC film. It can also be seen from the figure that after annealing at 400 °C, although the internal stress of the films is released, the critical load (Lc_1) decreases, which is due to the graphitization and decrease of hardness caused by elevated temperature. Due to the excellent thermal stability of SiOx-DLC-2 film, the critical load (Lc_1) decreases most weakly. The above analysis of the residual stress and adhesion of the films show that Si/O co-doping reduces the fraction of highly strained C—C bonds in a-C:H:Si:O films. The disorder of the a-C:H films present in the amorphous structure gives rise to a large faction of tensile strained C—C sp^3 bonds. Strained C—C sp^3 bonds have the lower strength and are more likely to break upon providing thermal energy and lead to an increase in the fraction of sp^2 C. The presence of C—Si bonds with longer equilibrium bond length (185 p.m. for C—Si and 154 p.m. for C—C) allows a-C:H:Si:O films to accommodate more structural disorder without the inclusion of many strained C—C sp^3 bonds (C—C bond with a length greater than 1.6 Å) [43,44].

4. Conclusion

a-C:H and a-C:H:Si:O films are prepared by PECVD with C_2H_2 and HMDSO. The Si/O co-doping reduces the degree of graphitization of a-C:H films after thermal annealing. After annealing at 400 °C, the decrease rate of sp^3 fraction of a-C:H film is 14.2%, while the a-C:H:Si:O (0.93 at.% Si) film is 8.16% and the a-C:H:Si:O (3.62 at.% Si) film is 6.8%. After annealing at 500 °C, The a-C:H:Si:O films are complete and the a-C:H film completely peels off from the substrate. A comparative analysis of the structure and residual stress of the two kinds of films is conducted. The higher thermal stability of a-C:H:Si:O compared to a-C:H derives from the reason: Silicon can be incorporated into carbon network contributing to produce C—Si sp^3 bonds which remains stable at high temperature, and reducing the fraction of highly strained C—C sp^3 bonds which are more likely to break upon providing thermal energy. Through the co-doping of Si/O elements, the hardness and critical load of a-C:H films at high temperature are greatly improved, which is expected to expand the application of DLC films.

CRediT authorship contribution statement

Dong Zhang: Conceptualization, Formal analysis, Data curation, Writing - original draft. **Shuyu Li**: Formal analysis, Methodology, Data curation. **Xiao Zuo**: Investigation. **Peng Guo**: Investigation. **Peiling Ke**: Validation. **Aiying Wang**: Supervision, Project administration.

Declaration of competing interest

The authors declare that they have no known competing financial interests or personal relationships that could have appeared to influence the work reported in this paper.

Acknowledgement

This work was financial supported by CAS Interdisciplinary Innovation Team (292020000008), K.C. Wong Education Foundation (GJTD-2019-13), and Ningbo Science and Technology Innovation Project (2018B10014).

References

[1] C.P.O. Treutler, Industrial use of plasma-deposited coatings for components of automotive fuel injection systems, Surf. Coat. Technol. 200 (2005) 1969–1975.
[2] K. Bewilogua, D. Hofmann, History of diamond-like carbon films from first experiments to worldwide applications, Surf. Coat. Technol. 242 (2014) 214–225.
[3] D. Caschera, P. Cossari, F. Federici, S. Kaciulis, A. Mezzi, G. Padeletti, D.M. Trucchi, Influence of PECVD parameters on the properties of diamond-like carbon films, Thin Solid Films 519 (2011) 4087–4091.
[4] J.J. Wang, J.B. Pu, G.G. Zhang, L.P. Wang, Interface architecture for superthick carbon-based films toward low internal stress and ultrahigh load-bearing capacity, ACS Appl. Mater. Interfaces 5 (2013) 5015–5024.
[5] M. Ban, T. Hasegawa, Internal stress reduction by incorporation of silicon in diamond-like carbon films, Surf. Coat. Technol. 162 (2003) 1–5.
[6] M. Grischke, K. Bewilogua, K. Trojan, H. Dimigen, Application-oriented modifications of deposition processes for diamond-like-carbon-based coatings, Surf. Coat. Technol. 74-75 ((1995) 739.
[7] D.R. Tallant, J.E. Parmeter, M.P. Siegal, R.L. Simpson, The thermal stability of diamond like carbon, Diam. Relat. Mater. 4 (1995) 191–199.
[8] J.C. Knight, T.F. Page, H.W. Chandler, Thermal instability of the microstructure and surface mechanical properties of hydrogenated amorphous carbon films, Surf. Coat. Technol. 49 (1991) 519–529.
[9] J. Robertson, Diamond-like amorphous carbon, Mater. Sci. Eng. R 37 (2002) 129–281.
[10] R. Hatada, K. Baba, S. Flege, W. Ensinger, Long-term thermal stability of Si-containing diamond-like carbon films prepared by plasma source ion implantation, Surf. Coat. Technol. 305 (2016) 93–98.
[11] H. Nakazawa, R. Kamata, S. Miura, S. Okuno, Effects of frequency of pulsed substrate bias on structure and properties of silicon-doped diamond-like carbon films by plasma deposition, Thin Solid Films 574 (2015) 93–98.
[12] G.M. Yu, Z.B. Gong, B.Z. Jiang, D.L. Wang, C.N. Bai, J.Y. Zhang, Superlubricity for hydrogenated diamond like carbon induced by thin MoS_2 and DLC layer in moist air, Diam. Relat. Mater. 102 (2020) 107668.
[13] H. Zhou, Q.Y. Hou, T.Q. Xiao, Y.D. Wang, B. Liao, X. Zhang, The composition, microstructure and mechanical properties of Ni/DLC nanocomposite films by filtered cathodic vacuum arc deposition, Diam. Relat. Mater. 75 (2017) 96–104.
[14] J. Huang, L.P. Wang, B. Liu, S.H. Wan, Q.J. Xue, In vitro evaluation of the tribological response of Mo-doped graphite-like carbon film in different biological media, ACS Appl. Mater. Interfaces 7 (2015) 2772–2783.
[15] N. Dwivedi, S. Kumar, J.D. Carey, R.K. Tripathi, H.K. Malik, M.K. Dalai, Influence of silver incorporation on the structural and electrical properties of diamond-like carbon thin films, ACS Appl. Mater. Interfaces 5 (2013) 2725–2732.
[16] Q.Z. Wang, F. Zhou, Z.F. Zhou, Y. Yang, C. Yan, C.D. Wang, W.J. Zhang, L.K.Y. Li, I. Bello, S.T. Lee, Influence of Ti content on the structure and tribological properties

of Ti-DLC coatings in water lubrication, Diam. Relat. Mater. 25 (2012) 163–175.
[17] S.C. Ray, W.F. Pong, P. Papakonstantinou, Iron, nitrogen and silicon doped diamond like carbon (DLC) thin films: a comparative study, Thin Solid Films 610 (2016) 42–47.
[18] X.W. Li, P. Guo, L.L. Sun, A.Y. Wang, P.L. Ke, Ab initio investigation on Cu/Cr codoped amorphous carbon nanocomposite films with giant residual stress reduction, ACS Appl. Mater. Interfaces 7 (2015) 27878–27884.
[19] X.W. Li, L.L. Sun, P. Guo, P.L. Ke, A.Y. Wang, Structure and residual stress evolution of Ti/Al, Cr/Al or W/Al co-doped amorphous carbon nanocomposite films: insights from ab initio calculations, Mater. Des. 89 (2016) 1123–1129.
[20] Y. Zhou, P. Guo, L.L. Sun, L.L. Liu, X.W. Xu, W.X. Li, X.W. Li, K.R. Lee, A.Y. Wang, Microstructure and property evolution of diamond-like carbon films co-doped by Al and Ti with different ratios, Surf. Coat. Technol. 361 (2019) 83–90.
[21] L.L. Sun, X. Zuo, P. Guo, X.W. Li, P.L. Ke, A.Y. Wang, Role of deposition temperature on the mechanical and tribological properties of Cu and Cr co-doped diamond-like carbon films, Thin Solid Films 678 (2019) 16–25.
[22] L.L. Sun, P. Guo, P.L. Ke, X.W. Li, A.Y. Wang, Synergistic effect of Cu/Cr co-doping on the wettability and mechanical properties of diamond-like carbon films, Diam. Relat. Mater. 68 (2016) 1–9.
[23] S. Jana, S. Das, D. De, U. Gangopadhyay, P. Ghosh, A. Mondal, Effect of annealing on structural and optical properties of diamond-like nanocomposite thin films, Appl. Phys. A-Mat. Sci. Pro. 114 (2014) 965–972.
[24] F.G. Sen, X. Meng-Burany, M.J. Lukitsch, Y. Qi, A.T. Alpas, Low friction and environmentally stable diamond-like carbon (DLC) coatings incorporating silicon, oxygen and fluorine sliding against aluminum, Surf. Coat. Technol. 215 (2013) 340–349.
[25] D. Franta, I. Ohlidal, V. Bursikova, L. Zajikova, Optical properties of diamond-like carbon films containing SiOx, Diam. Relat. Mater. 12 (2003) 1532–1538.
[26] S.M. Baek, T. Shirafuji, N. Saito, O. Takai, Adhesion property of SiOx-doped diamond-like carbon films deposited on polycarbonate by inductively coupled plasma chemical vapor deposition, Thin Solid Films 519 (2011) 6678–6682.
[27] S. Bhowmick, A. Banerji, M.J. Lukitsch, A.T. Alpas, The high temperature tribological behavior of Si, O containing hydrogenated diamond-like carbon (a-C:H/a-Si:O) coating against an aluminum alloy, Wear 330 (2015) 261–271.
[28] F. Mangolini, J.B. McClimon, J. Segersten, J. Hilbert, P. Heaney, J.R. Lukes, R.W. Carpick, Silicon oxide-rich diamond-like carbon: a conformal, ultrasmooth thin film material with high thermo-oxidative stability, Adv. Mater. Interfaces 6 (2019) 1801416.
[29] J. Lanigan, H. Zhao, A. Morina, J. Hilbert, P. Heaney, J.R. Lukes, R.W. Carpick, Tribochemistry of silicon and oxygen doped, hydrogenated diamond-like carbon in fully-formulated oil against low additive oil, Tribo. Inter. 82 (2015) 431–442.
[30] N. Kumar, S.A. Barve, S.S. Chopade, R. Kar, N. Chand, S. Dash, A.K. Tyagi, D.S. Patil, Scratch resistance and tribological properties of SiOx incorporated diamond-like carbon films deposited by r.f. plasma assisted chemical vapor deposition, Tribo. Inter. 84 (2015) 124–131.
[31] C. Casiraghi, A.C. Ferrari, J. Robertson, Raman spectroscopy of hydrogenated amorphous carbons, Phys. Rev. B 72 (2005) 085401.
[32] A.C. Ferrari, J. Robertson, Interpretation of Raman spectra of disordered and amorphous carbon, Phys. Rev. B 61 (2000) 14095–14107.
[33] A.C. Ferrari, J. Robertson, Resonant Raman spectroscopy of disordered, amorphous, and diamond like carbon, Phys. Rev. B 64 (2001) 075414.
[34] W.J. Yang, Y.H. Choa, T. Sekino, K.B. Shim, K. Niihara, K.H. Auh, Tribological evaluation of Si-O containing diamond-like carbon films, Surf. Coat. Technol. 162 (2003) 183–188.
[35] L.K. Randeniya, A. Bendavid, P.J. Martin, M.S. Amin, E.W. Preston, F.S.M. Ismail, S. Coe, Incorporation of Si and SiOx into diamond-like carbon films: impact on surface properties and osteoblast adhesion, Acta Biomater. 5 (2009) 1791–1797.
[36] S. Meskinis, R. Gudaitis, K. Slapikas, S. Tamulevicius, M. Andrulevicius, A. Guobiene, J. Puiso, G. Niaura, Ion beam energy effects on structure and properties of SiOx doped diamond-like carbon films, Surf. Coat. Technol. 202 (2008) 2328–2331.
[37] L.K. Randeniy, A. Bendavid, P.J. Martin, M.S. Amin, E.W. Preston, Molecular structure of SiOx-incorporated diamond-like carbon films; evidence for phase segregation, Diam. Relat. Mater. 18 (2009) 1167–1173.
[38] J.C. Damasceno, S.S. Camargo, Plasma deposition and characterization of silicon oxide-containing diamond-like carbon films obtained from CH_4:SiH_4:O_2 gas mixtures, Thin Solid Films 516 (2008) 1890–1897.
[39] A. Tamuleviciene, V. Kopustinskas, G. Niaura, S. Meskinis, S. Tamulevicius, Multiwavelength Raman analysis of SiOx and N containing amorphous diamond like carbon films, Thin Solid Films 581 (2015) 86–91.
[40] W.J. Yang, Y.H. Choa, T. Sekino, S. Meskinis, S. Tamulevicius, Thermal stability evaluation of diamond-like nanocomposite coatings, Thin Solid Films 434 (2003) 49–54.
[41] J.J. Wang, J.B. Pu, G.G. Zhang, L.P. Wang, Tailoring the structure and property of silicon-doped diamond-like carbon films by controlling the silicon content, Surf. Coat. Technol. 235 (2013) 326–332.
[42] J. Hilbert, F. Mangolini, J.B. McClimon, J.R. Lukes, R.W. Carpick, Si doping enhances the thermal stability of diamond-like carbon through reductions in carbon-carbon bond length disorder, Carbon 131 (2018) 72–78.
[43] F. Mangolini, J. Hilbert, J.B. McClimon, J.R. Lukes, R.W. Carpick, Thermally induced structural evolution of silicon- and oxygen-containing hydrogenated amorphous carbon: a combined spectroscopic and molecular dynamics simulation investigation, Langmuir 34 (2018) 2989–2995.
[44] S.A. Barve, S.S. Chopade, R. Kar, N. Chand, M.N. Deo, A. Biswas, N.N. Patel, G.M. Rao, D.S. Patil, S. Sinha, SiOx containing diamond like carbon coatings: effect of substrate bias during deposition, Diam. Relat. Mater. 71 (2017) 63–72.